Marine and Petroleum Geology 45 (2013) 171–185

Contents lists available at SciVerse ScienceDirect

Marine and Petroleum Geology

journal homepage: www.elsevier.com/locate/marpetgeo

Review article

Induced seismicity and hydraulic fracturing for the recovery of hydrocarbons

Richard Davies [a,*], Gillian Foulger [a], Annette Bindley [a,1], Peter Styles [b]

[a] Durham Energy Institute, Department of Earth Sciences, Durham University, Science Labs, Durham DH1 3LE, UK
[b] School of Physical and Geographical Sciences, Keele University, Keele, Staffordshire ST5 5BG, UK

ARTICLE INFO

Article history:
Received 11 December 2012
Received in revised form
22 March 2013
Accepted 27 March 2013
Available online 22 April 2013

Keywords:
Induced
Unconventional
Seismic
Earthquake
Fracturing

ABSTRACT

We compile published examples of induced earthquakes that have occurred since 1929 that have magnitudes equal to or greater than 1.0. Of the 198 possible examples, magnitudes range up to 7.9. The potential causes and magnitudes are (a) mining (M 1.6–5.6); (b) oil and gas field depletion (M 1.0–7.3); (c) water injection for secondary oil recovery (M 1.9–5.1); (d) reservoir impoundment (M 2.0–7.9); (e) waste disposal (M 2.0–5.3); (f) academic research boreholes investigating induced seismicity and stress (M 2.8–3.1); (g) solution mining (M 1.0–5.2); (h) geothermal operations (M 1.0–4.6) and (i) hydraulic fracturing for recovery of gas and oil from low-permeability sedimentary rocks (M 1.0–3.8).

Reactivation of faults and resultant seismicity occurs due to a reduction in effective stress on fault planes. Hydraulic fracturing operations can trigger seismicity because it can cause an increase in the fluid pressure in a fault zone. Based upon the research compiled here we propose that this could occur by three mechanisms. Firstly, fracturing fluid or displaced pore fluid could enter the fault. Secondly, there may be direct connection with the hydraulic fractures and a fluid pressure pulse could be transmitted to the fault. Lastly, due to poroelastic properties of rock, deformation or 'inflation' due to hydraulic fracturing could increase fluid pressure in the fault or in fractures connected to the fault. The following pathways for fluid or a fluid pressure pulse are proposed: (a) directly from the wellbore; (b) through new, stimulated hydraulic fractures; (c) through pre-existing fractures and minor faults; or (d) through the pore network of permeable beds or along bedding planes. The reactivated fault could be intersected by the wellbore or it could be 10s to 100s of metres from it.

We propose these mechanisms have been responsible for the three known examples of felt seismicity that are probably induced by hydraulic fracturing. These are in the USA, Canada and the UK. The largest such earthquake was M 3.8 and was in the Horn River Basin, Canada. To date, hydraulic fracturing has been a relatively benign mechanism compared to other anthropogenic triggers, probably because of the low volumes of fluid and short pumping times used in hydraulic fracturing operations. These data and analysis should help provide useful context and inform the current debate surrounding hydraulic fracturing technology.

1. Introduction

It has been known since the 1960s that earthquakes can be induced by fluid injection. At that time, military waste fluid was injected into a 3671-m-deep borehole at the Rocky Mountain Arsenal, Colorado (e.g., Hsieh and Bredehoeft, 1981). This induced the so-called 'Denver earthquakes'. They ranged up to M 5.3, caused extensive damage in nearby towns, and as a result, use of the well was discontinued in 1966. Despite the importance of induced seismicity, only a few holistic reviews have been published (e.g., Nicholson, 1992; Gupta, 2002; Li et al., 2007). Compilations often focus on selected mechanisms although there are notable exceptions (National Academy of Sciences, 2012).

Recently, the attention of regulators, agencies and the general public has been drawn to induced seismicity linked to the hydraulic fracturing of low-permeability sedimentary rocks such as 'tight' sandstones and shale, for oil and gas exploration and production. Hydraulic fractures are stimulated to increase the surface area of

* Corresponding author. Tel.: +44 7770 704198.
E-mail address: richard.davies@dur.ac.uk (R. Davies).
[1] Present address: Working Smart Ltd, Lynton House, Station Approach, Woking GU22 7PY, UK.

0264-8172/$ – see front matter © 2013 Elsevier Ltd. All rights reserved.
http://dx.doi.org/10.1016/j.marpetgeo.2013.03.016

rock which is connected to the wellbore. This is achieved by pumping water, proppant and chemicals during multiple fracture stages, a process known as 'fracking' (e.g., King, 2010). After pumping ceases the injected fluid is allowed to flowback to the surface and can be disposed of by reinjection or processing. Although hydraulic fracturing has been carried out since the 1940s, the combination of multiple stages of fracturing in horizontal wells in shale and tight sandstones and the widespread deployment of this technology did not start until the 1990s (e.g., Curtis, 2002).

During or soon after hydraulic fracturing there may be an increase in fluid pressure along a fault plane, which, if critically stressed, can be reactivated inducing seismicity (Fig. 1a and b). A thorough review of the history of induced seismicity caused by a variety of mechanisms including hydraulic fracturing is timely as it places the magnitudes and frequency of hydraulic-fracturing-triggered seismicity into context. We introduce the theory behind how earthquakes are induced, review the context of global induced seismicity since 1929, and discuss the evidence that faults are being reactivated as a result of hydraulic fracturing and the processes by which this could be occurring.

1.1. Earthquakes

All rock masses that experience progressively changing stress are potentially seismogenic, i.e., capable of producing earthquakes. Progressive loading of stress by tectonic plate movements is the primary geological earthquake-inducing process. It results in intense deformation at the boundaries of plates, which are the most active earthquake zones. Plates are not absolutely rigid and the effect of their motions is transmitted into their interiors. There, lower-level, intraplate deformation occurs. This is sometimes localized in rift zones, e.g., the East African rift, and sometimes distributed throughout broad regions, e.g., Britain, mainland Europe, and the Basin and Range Province, western U.S.A. (Sykes and Sbar, 1973).

Fluids play a critical role in triggering seismicity in many different geological scenarios. Earthquake activity accompanies volcanic activity, and liquid magma is involved in those cases, e.g., at Yellowstone, USA. Occasionally, large earthquakes are accompanied by significant changes in groundwater, e.g., changes in the level of the water table. Usually, however, there is no direct evidence of fluid involvement. Nevertheless, fluids must lubricate fault surfaces that slip in earthquakes because otherwise friction on the fault plane would be too large to be overcome at the failure energy levels observed. This conjecture is supported by the absence of a large heat flow anomaly above the San Andreas fault zone, which would inevitably be generated by the friction of dry rock surfaces slipping past each other (Lachenbruch and Sass, 1980).

Artificially injecting fluids into the Earth's crust induces earthquakes (e.g., Green et al., 2012). Fluid injection not only perturbs stress (Fig. 1b) (Scholz, 1990) and creates new fractures, but it also potentially introduces pressurised fluids into pre-existing fault zones, causing slip to occur earlier than it would otherwise have done naturally (Fig. 1a and b).

1.2. Earthquake sizes

Earthquakes range in magnitude from a maximum of ~10 down to arbitrarily small values. In the most sensitive microearthquake monitoring experiments, the lower magnitude limit of earthquakes that are reported is approximately M −3. Although traditional earthquake magnitudes are a familiar measure to most people, they are an empirical measure and no longer fit for modern purposes. They have thus been superseded by seismic moment, a measure that has physical meaning.

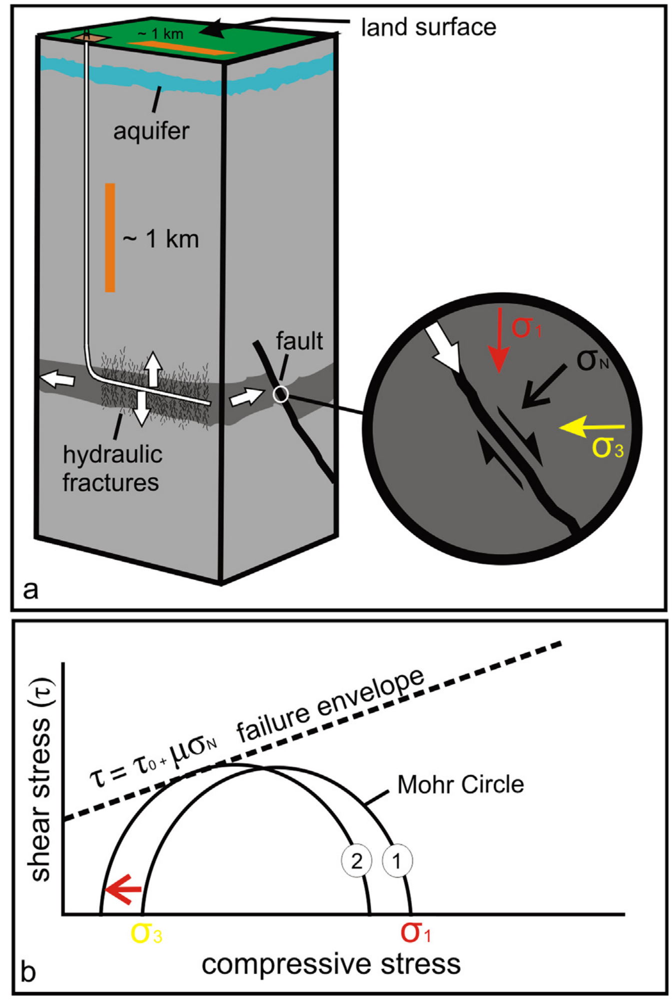

Figure 1. Induced seismicity caused by hydraulic fracturing. (a) Cartoon of a well drilled vertically and then horizontally into fine-grained, low-permeability strata (dark grey), which are offset by a normal fault (thick black line). Fluid, or a fluid pressure pulse, can be transmitted into a nearby or intersecting, critically stressed fault (white arrows). Compressive stresses σ_1, σ_2, and σ_3 act upon the fault. In this case σ_1 is depicted as being vertical, σ_2 is horizontal (out of the page and not shown), and σ_N is the normal stress acting on the fault plane. Failure occurs when the shear stress (τ) is higher than the sum of the shear strength (τo) and frictional stress on the fault plane ($\mu\sigma_N$), where μ is the coefficient of friction. (b) A Mohr diagram for the fault plane. Mohr Circle 1 represents σ_1 and σ_3 for the critically stressed fault plane prior to hydraulic fracturing. It is therefore located close to the Mohr failure envelope. During hydraulic fracturing, or during shut in of the well before flowback, the fluid pressure within the fault zone could increase. This could occur due to transmission of a fluid pressure wave or because hydraulic fracturing fluid or pore fluid enters the fault increasing fluid pressure. This causes a reduction in the compressive stress, σ_1 and σ_3, so the Mohr circle shifts to the left (red arrow, Mohr Circle 2), intersects the failure envelope, shear failure occurs, and if this is over a significant length of the fault, there is the potential for felt seismicity.

In the past, many magnitude scales were proposed to suit convenience in different situations, and several are still in widespread use. Magnitudes are calculated from measurements made directly from recorded seismograms, such as wave amplitudes or durations. Magnitude formulae usually take into account the epicentral distance of the earthquake from the recording station, but they ignore many other factors such as the hypocentral depth and the structure of the Earth between the source and the recorder. As a result, magnitude is not a measure of source physics, but of seismogram characteristics. Different magnitudes are typically obtained by analysing seismograms recorded at different seismic stations, or by applying different magnitude scales to the same seismogram. Examples of different magnitude scales are the local magnitude scale (M_L – popularly known as the "Richter" magnitude scale), the surface-wave magnitude scale (m_S), and the duration magnitude scale (M_D). A further complication is that the type of instrument used may be included in the magnitude scale definition. For example, local magnitude is defined as applying to measurements made from seismograms recorded on Wood-Anderson seismographs. These instruments are now obsolete, so the "Richter" magnitudes commonly reported nowadays are not valid, for this reason alone.

A rigorous way of estimating earthquake size is by using seismic moment. This is the low-frequency scalar moment, M_0, and it is a measure of size based on the fundamental physics of the earthquake source. M_0 varies by over 18 orders of magnitude, and thus it is conventional to express it using an empirically derived logarithmic moment–magnitude relationship that yields numbers similar to typical magnitudes. This formula is:

$$M_W = 2/3 \log M_0 - 10.7$$

where M_0 is measured in dyne-cm (Hanks and Kanamori, 1979; Kanamori, 1977). The moment magnitude (M_W) of an earthquake is theoretically the same regardless of where the earthquake was measured, the type of recording instrument, structure along the wavepaths, or which stations are used. If earthquake size is an important parameter it is crucial to use moment magnitude. Only then can the sizes of earthquakes from different regions or time periods be meaningfully compared.

If moments are unavailable, the next best thing is to use the same type of magnitude, e.g., M_L or M_D. Estimates for the same earthquake made using different magnitude scales may vary by one, or even as much as two, magnitude units.

1.3. Earthquake numbers

Earthquakes result from brittle failure of the Earth's crust. They exhibit a log normal frequency distribution (Gutenberg and Richter, 1944). The frequency-magnitude slope of earthquake sequences is usually approximately unity, meaning that for every reduction of one magnitude unit, ten times as many earthquakes occur (Gutenberg and Richter, 1944). The seismic rate for the world is approximately one magnitude 9 earthquake per decade, one magnitude 8 per year, 10 magnitude 7s, 100 magnitude 6s and so on. The stress released by an earthquake is, however, approximately 30 times that released by an earthquake one magnitude unit smaller. From this is easy to see why large earthquakes cannot be prevented by inducing many smaller earthquakes. The fractal nature of earthquakes induced by human operations is not fundamentally different from that of natural earthquakes, and no case has ever been reported where several tens of earthquakes of a given magnitude have been induced without also producing events a magnitude unit larger.

The number of earthquakes detected by a seismic network is dependent on observational factors, e.g., the proximity of the nearest seismic station and the quality of the installation. The closer the station and the higher-quality the installation, the lower will be the magnitude detection threshold and the larger the number of earthquakes reported. Improvement of a network such that it detected earthquakes one magnitude unit lower, e.g., by adding additional stations close to the activated zone, would immediately increase the numbers of earthquakes reported by an order of magnitude. Thus, the number of earthquakes reported must be taken in context. For example, a report that the number of earthquakes observed at one project was greater than the number observed at another project is meaningless unless the monitoring conditions were identical.

Earthquake magnitudes follow a power law distribution described by the Gutenberg–Richter relationship (Gutenberg and Richter, 1944):

$$\log N = a - bM,$$

where N is the number of earthquakes with magnitude greater than or equal to magnitude M, and a and b are constants.

1.4. Induced earthquakes

A fault slips when the normal stress across a fault plane drops to a sufficiently low level that the shear stress overcomes the static friction on the fault surface. This is expressed by the Mohr diagram (Fig. 1b). A fault can be brought to a critical state either by increasing the shear stress, e.g., by plate motions or surface loading, or by decreasing the normal stress that clamps the fault surfaces together. The latter could be caused by processes such as stretching, exhumation and erosion and by increasing the fluid pressure in the fault zone.

Stress is perturbed, and earthquakes induced, by a number of anthropogenic activities that change the loading state of the Earth's crust. These include the removal of subsurface volume by mining the solid rock or the extraction of oil and gas. Mine-quakes are a significant safety hazard and are common for example in the UK and South Africa. Some mining operations, e.g., deep gold mines in South Africa, are seismically monitored for safety reasons. Depleted hydrocarbon reservoirs are often seismogenic, as reservoirs collapse in response to the removal of pore fluids.

The injection of fluids into the subsurface is an increasingly common activity. It is done to dispose of waste water or chemicals, to flush hydrocarbons out of oil reservoirs, to fracture shale for gas and oil extraction and to introduce water into geothermal reservoirs to create permeability and for circulation of hot fluid. Because of the importance of managing induced earthquakes, the factors that could affect the size of the largest earthquakes induced by fluid-injection are of critical interest. Candidate operational parameters include the temperature and volume of the fluid injected, and its type, phase, injection rate, pressure and depth below the surface. The pre-existing stress- and fracture-state of area, i.e., whether the area contains large faults and is tectonically active, may also be important. Fluid injections in stable continental interiors where differential stress levels are low and static, and there is no history of seismicity, are likely be less seismogenic than injections in areas of active tectonics that already have a high natural seismic rate and are thus critically stressed even before injection commences. Sometimes, induced seismicity can reveal the presence of previously unknown faults. Correlations of various operational and seismic parameters have been measured in an attempt to explore possible mitigating operational approaches.

2. History of induced seismicity

Since 1993 there have been seven generally accepted criteria that must be met before fault reactivation is considered to have an anthropogenic origin (Davis and Frohlich, 1993). These are:

1. Are these events the first known earthquakes of this character in the region?
2. Is there a clear correlation between injection and seismicity?
3. Are epicentres near wells (within 5 km)?
4. Do some earthquakes occur at or near injection depths?

5. If not, are there known geologic structures that may channel flow to sites of earthquakes?
6. Are changes in fluid pressures at well bottoms sufficient to encourage seismicity?
7. Are changes in fluid pressures at hypocentral distances sufficient to encourage seismicity?

The literature on induced seismicity dates back to 1933 (Gupta, 1985; Rothé, 1970), well before the proposal by Davis and Frohlich (1993) of these criteria. In this paper we compile all potential examples of induced seismicity, many of which did not use these criteria. The total of 198 possible examples, come from 66 published papers and reports (Tables 1–3). Because we only use published examples, our database is not comprehensive. For instance, we are aware of many unpublished examples of induced earthquakes associated with the mining industry in the UK, but it is beyond the scope of this review paper to analyse unpublished datasets. Lastly, in cases where a swarm of earthquakes thought to be induced is reported, we have only recorded the magnitude of the largest event.

We subdivide the seismicity by likely trigger mechanism into: (a) mine subsidence, (b) oil and gas field depletion, (c) fluid injection for secondary oil recovery, (d) research-related projects, (e) waste-water disposal, (f) solution mining, (g) Enhanced Geothermal Systems (EGS) operations, (h) reservoir impoundment, (i) groundwater extraction, and (j) hydraulic fracturing for recovery of hydrocarbons from shale. We briefly review (a)–(i), and consider (j) in more detail.

2.1. Mine subsidence

Earthquakes induced by mine subsidence are some of the most widely studied. They are often due to collapse of mine workings (e.g., Bennett et al., 1996; Hubert et al., 2006; Li et al., 2007). These earthquakes range from M 1.6 to 5.6 (Table 1). Often the only damage they cause is to the mines and miners working in them, but they have been known to damage the wider community (Li et al., 2007).

2.2. Oil and gas field depletion

Earthquakes are caused by compaction of reservoirs as a result of hydrocarbon extraction (e.g., Suckale, 2009). The flexure of the overburden generates shear stresses that can induce slip along weak shale strata (e.g., Hamilton et al., 1992). At the Lacq gas field (southwest France) 1639 earthquakes were detected around the field in the magnitude range M 1.9 to 6 (Bardainne et al., 2008). In 1976, 1984 there were M 7.0 events at Gazli, Uzbekistan. The area around Gazli had been aseismic until these events. It is uncertain that these events were induced, but several criteria indicate that these are the largest examples of earthquakes induced by gas extraction from a conventional gas field (Table 2).

2.3. Fluid injection for secondary oil recovery

Water is injected into oil fields to increase the percentage of oil recovered and it can enter faults reducing normal stress and allowing reactivation. Fluid injection for oil recovery also maintains reservoir pressure and reduces or eliminates the compaction effects if that pressure is communicated effectively throughout the reservoir. Davis and Pennington (1989) documented events with $M_b - 4.3$ to $M_L - 5$ between 1974 and 1982 at the Cogdell oil field in West Texas, USA. Cesca et al. (2011) document an example of a 4.3 M event at the Ekofisk field (North Sea, UK), probably caused by water injection. Magnitudes of earthquakes range from M 1.9–5.1 (Table 2).

2.4. Research-related projects

Approximately 400 earthquakes occurred in association with the German Continental Deep Drilling Program, which included a borehole drilled to 9.1 km depth. They occurred at an average depth of 8.8 km and are thought to have been induced by injection of brine into a 70-m-thick open-hole section near the bottom of the borehole. One conclusion of this work was that critically stressed, permeable fault zones exist in the crust, even at great depth and temperature (Zoback and Harjes, 1997). The event magnitudes ranged from 2.8–3.1 (Table 2).

2.5. Waste-water disposal

Frohlich et al. (2011) concluded that the most likely cause of an increase in seismicity in the Dallas Fort Worth area, USA, with events of up to M 3.6, was probably the result of injecting waste flowback water derived from the hydraulic fracturing of shale for gas production. The depth and location of seismicity were close to recent waste water injection activity. Magnitudes for a range of different waste water injection activities are 2.0–5.3 (Table 2).

2.6. Solution mining

Solution mining involves drilling wells into underground salt deposits and injecting water into them to dissolve the salt. The earliest reported induced earthquake is attributed to this operational technique (see Pechmann et al., 1995). That earthquake occurred in Attica (New York, USA) in 1929, and had a magnitude of M 5.3.

2.7. Enhanced Geothermal Systems (EGS) operations

The US$60 million Basel, Switzerland Enhanced Geothermal Systems project involved creating a fracture network in hot rock, through which fluid could be circulated to extract heat. Earthquakes with magnitudes up to M_L 2.9 began to occur six days into the main hydraulic fracturing operation (e.g., Häring et al., 2008). This activity exceeded a pre-decided injection-cessation threshold, but even though pumping was stopped, several more earthquakes with magnitudes exceeding M_L 3.0 occurred over the following two months. In total, 13,500 earthquakes were recorded, nine of which were of M_L 2.5 or larger (Table 2).

2.8. Reservoir impoundment

Reservoir impoundment is a widely documented cause of induced earthquakes, and a significant review was carried out in 1985 (Gupta, 1985). The weight of water loading on the surface provides enough pressure to induce earthquakes (Carder, 1945). Magnitudes of recorded cases range from 1.0 to 7.9 (Table 3). There is dispute, however, as to whether the very large Wenchuan, China M 7.9 earthquake resulted from filling the reservoir, or whether it was a natural process (Ge et al., 2009 vs. Deng et al., 2010). It resulted in ~90,000 deaths and ~100,000 injuries (Gahalaut and Gahalaut, 2010). This issue is currently causing concern as the Three Gorges Dam on the Yangtze river fills, and induced earthquakes as large as M 6.5 there have been forecast (Lixin et al., 2012).

Table 1
Earthquakes induced by mining operations.

Mine	Location	Resource	Largest Earthquake			Reference
			Date	Magnitude	Magnitude type reported	
Trona Mines	Wyoming	Trona	1995	5.1	M_L	1
Newcastle	Australia	Coal	1989	5.6	M_o	2
Ural Mts	Russia		1995	4.4	M	2
	South Africa		1994	5.6	M	2
Kentucky	USA		1995	4	M	2
New York	USA		1994	3.6	M	2
Welkom	South Africa	Gold	1976	5.2	M_L	3
Klerksdorp	South Africa	Gold	1977	5.2	M_L	3
Carletonville	South Africa	Gold	1992	4.7	M_L	3
Klerksdorp	South Africa	Gold	2004	4.9	M_L	3
Klerksdorp	South Africa	Gold	2005	5.3	M_L	3
Saar	Germany	Coal	2008	4	M_L	4
Ruhr	Germany	Coal	2007	3.3	M_L	4
	UK	Coal	1986	2.8	M_L	5
Saarland	Germany	Coal	2008	4	M_L	6
Utah	USA	Coal	2000	2.2	M_L	7
Liaoning	China	Coal	1977	4.3	M	8
Copper Cliff North	Ontario, Canada		2008	3.8	M_o	9
Craig	Ontario, Canada		2007	2.2	M_o	9
Creighton	Ontario, Canada		2006	4.1	M_o	9
Fraser	Ontario, Canada		2008	2.4	M_o	9
Garson	Ontario, Canada		2008	3.3	M_o	9
Kidd Creek	Ontario, Canada		2009	3.8	M_o	9
Macassa	Ontario, Canada		2008	3.1	M_o	9
Nanshan	China	Coal	2001	3.7	M_L	10
Gangdong	China	Coal		2.3	M_L	10
Shengli	China	Coal	1978	2.8	M_L	10
Laohutai	China	Coal	1981	2.5	M_L	10
Wulong	China	Coal	2004	3.8	M_L	10
Taiji	China	Coal	1977	4.3	M_L	10
Benxi Caitun	China	Coal	2004	2.8	M_L	10
Mentougou	China	Coal	1994	4.2	M_L	10
Chengzi	China	Coal		3.4	M_L	10
Fangshan	China	Coal	1997	3	M_L	10
Jinhuagong	P China	Coal		2.1	M_L	10
Baidong	China	Coal	1983	2.7	M_L	10
Hauting	China	Coal		3.3	M_L	10
Taozhuang	China	Coal	1982	3.6	M_L	10
Shunyuan	China	Coal	2002	3.6	M_L	10
Sanhejian	China	Coal	2003	3.4	M_L	10
Weixi	China	Salt	1979	4.2	M_L	10
Zigong	China	Salt	1985	4.6	M_L	10
Louguanshan	China		1994	4.3	M_L	10
Chayuan	China	Coal	1987	4.3	M_L	10
Yanshitai	China	Coal	1987	4.3	M_L	10
Huachu	China	Coal	1982	4.1	M_L	10
Sijiaotian	China	Coal	1985	2.7	M_L	10
Liuzhi	China	Coal	1991	3.6	M_L	10
Dizong	China	Coal	1985	2.7	M_L	10
Bingshuijing	China	Coal	1991	3.6	M_L	10
Dayong	China	Coal	1991	3.1	M_L	10
Xifeng Nanshan	China	Coal	1991	3.1	M_L	10
Shanjiaocun	China	Coal	1997	3.1	M_L	10
Yueliangtian	China	Coal	1997	3.1	M_L	10
Dahebian	China	Coal	1985	2.8	M_L	10
Kaiyang	China	Phosphorus	1990	2.2	M_L	10
Meitanba	China	Coal	1991	2.8	M_L	10
Enkou	China	Coal	1976	2.9	M_L	10
Doulishan	China	Coal	1985	2.5	M_L	10
Qiaotouhe	China	Coal	1974	2.2	M_L	10
Shixiajiang	China	Coal	1991	1.6	M_L	10
Xindong	China	Coal	1994	3	M_L	10
Niumasi	China	Coal	1997	3.2	M_L	10
Dahuatang	China	Coal	1997	2.7	M_L	10
Qingshan	China	Pyrite	1996	2.6	M_L	10
Qixingjiezhen	China	Coal	1996	3.1	M_L	10
Xujiadong	China	Uranium	1998	3.4	M_L	10
Niwan	China	Gypsum	2003	2.8	M_L	10
Shuikoushan	China	Lead–Zinc		2	M_L	10
Yanguan	China	Coal	1988	2.5	M_L	10
Huayazi	China	Coal	1973	2.8	M_L	10

(*continued on next page*)

Table 1 (*continued*)

Mine	Location	Resource	Largest Earthquake			Reference
			Date	Magnitude	Magnitude type reported	
Huaibashi	China	Coal	1972	3.6	M_L	10
Wacang	China	Coal	1971	3.8	M_L	10
Western Deep Levels East	South Africa	Gold	1996	4	M_L	11
Wappingers Falls	New York, USA		1974	3.3	M	12
Reading	Pennsylvania, USA		1994	4.3	M	12
Belchatow	Poland	Coal	1980	4.6	M	12

1. Pechmann et al. (1995); 2. Bennett et al. (1996); 3. Hubert et al. (2006); 4. Bischoff et al. (2009); 5. Redmayne (1988); 6. Fritschen (2009); 7. Arabasz et al. (2005); 8. Zhong et al. (1997); 9. Vallejos and McKinnon (2011); 10. Li et al. (2007); 11. Amidzic et al. (1999); 12. Majer (2011). Gaps in this and subsequent tables are where information was not specified in the published source.

Table 2
Earthquakes induced by waste injection, oil and gas field depletion, pressure support for oil and gas fields, salt mining, hydraulic fracturing for shale gas exploitation and geothermal exploitation.

Project	Location	Resource	Activity	Largest Earthquake			Ref
				Year	Magnitude	Magnitude type reported	
Catoosa	Oklahoma, USA	Gas	Withdrawal	1956	4.7	M_L	1
East Durant	Oklahoma, USA	Gas	Withdrawal	1968	3.5	M_L	1
El Reno	Oklahoma, USA	Gas	Withdrawal		5.2	M_L	1
Flashing Field	Texas, USA	Gas	Withdrawal		3.4	M_L	1
Imogene Field	Texas, USA	Gas	Withdrawal	1984	3.9	M_L	1
War-Wink	Texas, USA	Gas	Withdrawal		3	M_L	1
Fashing	Texas, USA	Gas	Withdrawal	1993	4.3	M_b	2
Lacq	France	Gas	Withdrawal	1978	4.2	M_L	3
Gazli	Uzbekistan	Gas	Withdrawal	1976	7.3	M_L	4
Eleveld	Netherlands	Gas		1991	2.7	M_L	5
Snipe Lake	Alberta, Canada	Hydrocarbons	Secondary recovery	1970	5.1	M_L	1
Strachan	Alberta, Canada	Hydrocarbons	Secondary recovery	1974	4	M_L	1
Sleepy Hollow	Nebraska, USA	Hydrocarbons	Secondary recovery		2.9	M_L	1
Love Co	Oklahoma, USA	Hydrocarbons	Secondary recovery		1.9	M_L	1
Gobles Field	Ontario, USA	Hydrocarbons	Secondary recovery	1979	2.8	M_L	1
Cogdell Field	Texas, USA	Hydrocarbons	Secondary recovery	1989	5.3	M_L	1,6
Dollarhide	Texas, USA	Hydrocarbons	Secondary recovery		3.5	M_L	1
Dora Roberts	Texas, USA	Hydrocarbons	Secondary recovery		3	M_L	1
Kermit Field	Texas, USA	Hydrocarbons	Secondary recovery		4	M_L	1
Keystone	Texas, USA	Hydrocarbons	Secondary recovery		3.5	M_L	1
Monahans	Texas, USA	Hydrocarbons	Secondary recovery		3	M_L	1
Panhandle	Texas, USA	Hydrocarbons	Secondary recovery		3.4	M_L	1
Ward-Estes	Texas, USA	Hydrocarbons	Secondary recovery		3.5	M_L	1
Ward-South	Texas, USA	Hydrocarbons	Secondary recovery		3	M_L	1
Apollo Hendrick Field	Texas, USA	Hydrocarbons	Secondary recovery		2	M	7
	Iran	Hydrocarbons			6	M_L	5
Montebello	California, USA	Oil	Production	1987	5.9	M_L	1
Orcutt Field	California, USA	Oil	Production	1991	3.5	M_L	1
Wilmington	California, USA	Oil	Production		5.1	M_L	1
Richland	Illinois, USA	Oil	Production		4.9	M_L	1
Romashkinskoye	Russia	Oil	Production	1991	4	M_o	8
Renqiu	China	Oil	Production	1987	4.5	M_L	9
Xingtai	China	Oil	Production	1981	6	M_L	9
Hunt Field	Mississippi, USA	Oil	Secondary recovery	1978	3.6	M_L	1
East Texas	Texas, USA	Oil	Secondary recovery	1957	4.3	M_L	1
Ekofisk	North Sea, UK	Oil	Secondary recovery	2001	4.2	M_o	10
Barsa-Gelmes-Wishka	Turkmenistan	Oil	Secondary recovery		6	M_L	11
Akmaar	Netherlands	Oil	Withdrawal		3.5	M	12
Cleburne	Texas, USA	Oil	Withdrawal		2.8	M	13
Groningen Field	Netherlands	Oil	Withdrawal		3.2	M	14
Roswinkel	Netherlands	Oil	Withdrawal		3.4	M	14
Rotenburg	Germany	Oil	Withdrawal		4.5	M	13
Elsenbech	Germany	Other			5.8	M	13
Upper Silesian	Germany	Other			4.5	M	13
Rangely	Colorado, USA	Research	Research		3.1	M_L	1
Matsushiro	Japan	Research	Research	1970	2.8	M	15,16
KTB	Germany	Research	Research		2.8	M	17
Attica	New York, USA	Salt	Solution mining	1929	5.2	M_L	1
Dale	New York, USA	Salt	Solution mining	1971	1	M_L	1
Cleveland	Ohio, USA	Salt	Solution mining		3	M_L	1
Dallas-Fort Worth	Texas, USA	Shale Gas	Water disposal	2009	3.3	M	18
Ashtubla	Ohio, USA	Shale Gas	Water disposal	1987	3.6	M_L	1
Perry	Ohio, USA	Shale Gas	Water disposal		2.7	M_L	1

Table 2 (*continued*)

Project	Location	Resource	Activity	Largest Earthquake			Ref
				Year	Magnitude	Magnitude type reported	
Lancashire	UK	Shale Gas	Hydraulic fracturing	2011	2.3	M_o	19
Etsho and Kiwigana,	Canada	Shale Gas	Hydraulic fracturing	2009–2011	3.8	M_L	35
Eola Field	Oklahoma	Shale Gas	Hydraulic fracturing	2011	2.8	M	22
Cold Lake	Alberta, Canada	Waste	Disposal		2	M_L	1
El Dorado	Arizona, USA	Waste	Disposal		3	M_L	1,16
Denver	Colorado, USA	Waste	Disposal	1967	5.3	M_L	1,20
Lake Charles	Los Angeles, USA	Waste	Disposal		3.8	M_L	1
Paradox Valley	Colorado, USA	Waste	Disposal		4.3	M	21
Geysers	California, USA	Geothermal		1982	4.6	M_L	23
Rangely	Colorado, USA	Geothermal		1964	3.4	M_L	24
Basel	Switzerland	Geothermal		2006	3.4	M_L	25
Cooper Basin	Australia	Geothermal		2003	3.7	M_o	26
Soultz	France	Geothermal			2.7	M_L	27
Berlin	El Salvador	Geothermal		2003	4.4	M_o	28
Reykjanes	Iceland	Geothermal		2008	4	M_L	29
Larderello	Italy	Geothermal		1978	3.2	M_L	30
Fenton Hill	New Mexico, USA	Geothermal		1971	1	M	31
Bad Urach	Germany	Geothermal			1.8	M_o	32
Cesano	Italy	Geothermal			2	M_o	32
Krafla	Iceland	Geothermal			2	M_o	32
Landau	Germany	Geothermal			2.7	M_o	32
Latera	Italy	Geothermal			3	M_o	32
German Continental Deep Drilling Program	Germany	Geothermal			1.2	M_o	32
Monte Amiata	Italy	Geothermal			3.5	M_o	32
Mutnovsky	Russia	Geothermal			2	M	33
Ogachi	Japan	Geothermal			2	M	34
Rosemanowes	UK	Geothermal			2	M_o	32
Torre Alfina	Italy	Geothermal			3	M_o	32
Unterhaching	Germany	Geothermal			2.4	M_o	32

1. Nicholson (1992); 2. Davis et al. (1995); 3. Lahaie et al. (1998); 4. Mirzoev et al. (2009); 5. Roest and Kuilman (1994); 5. Jalali et al. (2008); 6. Davis and Pennington (1989); 7. Doser et al. (1992); 8. Galybin et al. (1998); 9. Genmo et al. (1995); 10. Ottermöller (2005); 11. Kouznetsov et al. (1994); 12. Giardini (2011); 13. Howe et al. (2010); 14. Van Eck et al. (2006); 15. Ohtake (1974); 16. Nicholson and Wesson (1990); 17. Zoback and Harjes (1997); 18. Frohlich et al. (2011); 19. de Pater and Baisch (2011); 20. Van Poollen and Hoover (1970); 21. Ake et al. (2005); 22. Holland (2011); 23. Julian et al. (1996); 24. Gibbs et al. (1973); 25. Häring et al. (2008); 26. Baisch et al. (2006); 27. Bourouis and Pascal (2007); 28. Majer et al. (2007); 29. Keiding et al. (2010); 30. Batini et al. (1985); 31. Phillips et al. (2002); 32. Evans et al. (2012); 33. Kugaenko et al. (2005); 34. Kaieda et al. (2010). 35. BC Oil and Gas Commission (2012). The 2011 M_w 5.7 earthquake sequence published by Keranen et al. (in press) is not included in the table and represents the largest earthquake triggered by waste water injection to be published to date.

Table 3
Earthquakes induced by surface reservoir construction and impoundment.

Reservoir	Location	Year of impoundment	Largest Earthquake			References
			Date	Magnitude	Magnitude type reported	
Marathon	Greece	1929	1938	5.7	M_L	1
Oued Fodda	Algeria	1932	1933	3	M_L	1, 2
Hoover	Nevada, USA	1935	1939	5	M_L	1, 2
Shasta	California, USA	1944	1944	3	M_L	1
Clark Hill	Indiana, USA	1952	1974	4.3	M_L	1
Eucumbene	Australia	1957	1959	5	M_L	1
Kariba	Zambia	1958	1963	6.2	M_L	1, 3
Kerr	North Carolina, USA	1958	1971	4.9	M_L	1
Camerillas	Spain	1960	1964	4.1	M_L	1
Canellas	Spain	1960	1962	4.7	M_L	1, 2
Kurobe	Japan	1960	1961	4.9	M_L	1
Koyna	India	1962	1967	6.3	M_L	1, 2
Monteynard	France	1962	1963	4.9	M_L	1, 2
Contra	Switzerland	1963	1965	3	M_L	1
Aswan Dam	Egypt	1964	1981	5.5	M_L	1
Benmore	New Zealand	1964	1966	5	M_L	1
Kremesta	Greece	1965	1966	6.3	M_L	1, 2, 4
Piastra	Italy	1965	1966	4.4	M_L	1
Grancarevo	Serbia	1967	1967	3	M_L	1
Oroville	Washington, USA	1967	1975	5.7	M_L	1
Blowering	Australia	1968	1973	3.5	M_L	1
Vouglans	France	1968	1971	4.4	M_L	1
Kastraki	Greece	1969	1969	4.6	M_L	1
Hendrik Verwoerd	South Africa	1970	1971	2	M_L	1
Kamafusa	Japan	1970	1970	3	M_L	1
Schlegeis	Austria	1970	1971	2	M_L	1

(continued on next page)

Table 3 (*continued*)

Reservoir	Location	Year of impoundment	Largest Earthquake			References
			Date	Magnitude	Magnitude type reported	
Jocassee	South Carolina, USA	1971	1975	3.2	M_L	1, 5, 6
Talbingo	Australia	1971	1973	3.5	M_L	1
Nurek	Tajikistan	1972	1972	4.6	M_L	1, 5
Emmonson	Switzerland	1973	1973	3	M_L	1
Keban	Turkey	1973	1973	3.5	M_L	1
Volta Grande	Brazil	1973	1974	4	M_L	1
Idukki	India	1975	1977	3.5	M_L	1
Manicouagan	Quebec Canada	1975	1975	4.1	M_L	1
Itezhitezhi	Zambia	1976	1978	4	M_L	1
Monticello	California, USA	1977	1979	2.8	M_L	1
Srinagarind	Thailand	1977	1983	5.9	M_L	1, 7
Toktogul	Kyrgyzstan	1977		2.5	M_L	1
Zipingpu	China	2006	2008	7.9	M_L	1, 8, 9, 10, 11

1: Gupta (1985); 2: Rothé (1970); 3: Gough and Gough (1970); 4: Stein et al. (1982); 5: Keith et al. (1982); 6: Zoback and Hickman (1982); 7: Chung and Liu (1992); 8: Gahalaut and Gahalaut (2010); 9: Lei et al. (2008); 10: Klose (2007); 11: Ge et al. (2009).

2.9. Groundwater extraction

González et al. (2012), suggest that stress induced by major groundwater extraction probably triggered the M_W 5.1 earthquake that occurred in Lorca, southeast Spain, 11th May 2011. This earthquake caused nine fatalities and considerable devastation for such a moderate event, principally because the focus was shallow at about 2–4 km depth.

Faults in the crust are in a state of frictional equilibrium under complex systems of stress, partly tectonic in this case through the interaction between the North African and Southern European areas, and also because of the weight of the overburden itself. Isostatic unloading and the associated elastic response of the crust and lithosphere is well known as a cause of seismicity, and much of NW Scotland's historic seismicity is associated with glacial unloading from the last ice sheet ca. 10,000 years ago. The Betic Cordillera is one of the most seismically active areas in the Iberian Peninsula and it is not surprising that the removal of 250 m of groundwater since 1960, a significant mass change over a short period of time, together with the many centimetres of subsidence caused by the consequential compaction, could provide the minor stress perturbation necessary to bring local faults to failure.

Figure 2 shows a graph of earthquake magnitude vs. frequency where magnitudes range from 1.0 to 7.9. This graph only documents examples of induced seismicity which have been published, and the hundreds of anecdotal mining-induced earthquakes with $M > 1$ in the UK, for example, are not included. Figure 2 shows that the most commonly reported induced earthquakes are M 3–4. The paucity of events of smaller magnitudes reflects lack of detection and reporting. Mining, oil- and gas-field depletion, reservoir impoundment, EGS wells, and waste water injection are the most frequently reported causes of induced seismicity.

3. Hydraulic fracturing

3.1. Operations

Exploration wells targeting low permeability sedimentary reservoirs, particularly in new exploration settings, are commonly drilled vertically and then hydraulically fractured. Production wells are typically deviated so that the borehole is strata-parallel through the reservoir (Fig. 1a). The production casing is perforated and hydraulic fractures are stimulated by injecting saline water with chemical additives. 'Proppant'– sand or synthetic ceramic spheres – is used to keep the fractures open (e.g. King, 2010). Hydraulic fracture stimulation from a horizontal borehole is usually carried out in multiple stages with fluids with known volumes and compositions (e.g., Bell and Brannon, 2011). Approximately 10–40% of the hydraulic fracturing fluid used flows back after stimulation. In some cases faulted areas of the reservoir are specifically targeted because there may be pre-existing fault and fracture permeability.

There are many good examples of hydraulic fracturing that has caused fault or fracture reactivation (e.g., Warpinski et al., 1998; Wolhart et al., 2005; Vulgamore et al., 2007; Maxwell et al., 2008; Cipolla et al., 2012). The seismicity is generally very low magnitude (<M 0) and typically not recorded above the noise level by traditional surface seismometer networks. Monitoring of fracture growth and fault reactivation is thus done using downhole geophone strings that are deployed within a few hundred metres of the hydraulic fracturing. Only by deploying sensors so close to the seismicity can data be collected of sufficient high quality that locations and other processing results can be calculated for these tiny events. Alternatively, massive surface arrays comprising hundreds

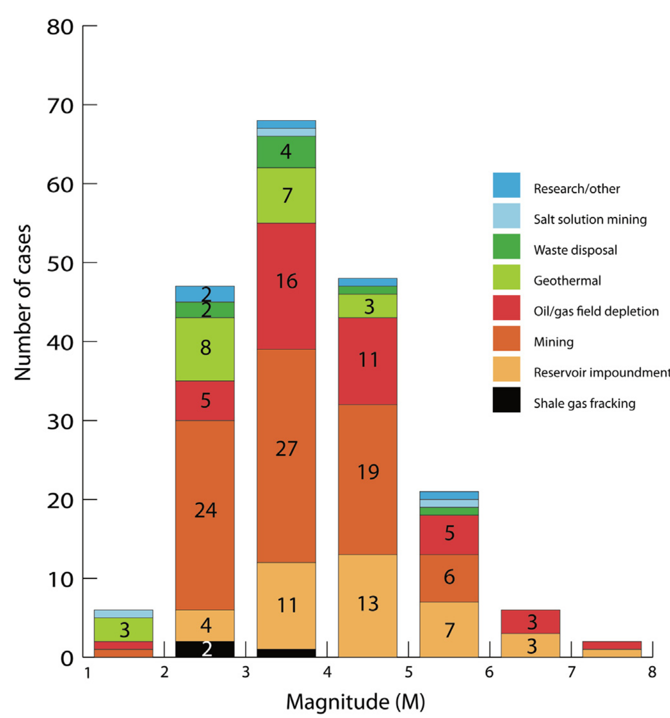

Figure 2. Frequency vs. magnitude for 198 published examples of induced seismicity (see Tables 1–3). The many examples of induced seismicity that are not published are not included on this graph.

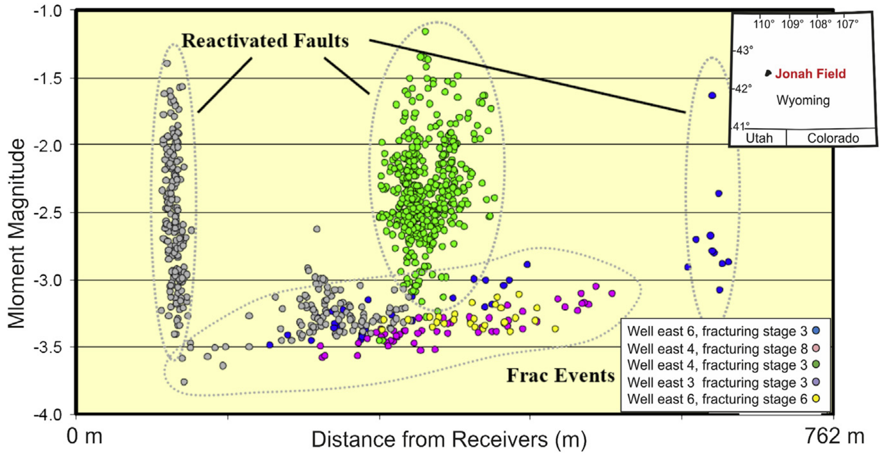

Figure 3. Moment magnitude vs. distance from seismic stations for induced hydraulic fracturing operations in a number of wells in the Jonah Field (Wyoming, USA – after Wolhart et al., 2005). The clustering of events with larger magnitudes is indicative of fault reactivation due to pumping of hydraulic fracturing fluid. Inset – location map.

or thousands of seismometers are deployed, so the signal-to-noise ratio can be enhanced by stacking the seismograms (Grechka, 2010; Gei et al., 2011).

Most of the criteria proposed by Davis and Frohlich (1993) for induced seismicity are fulfilled for seismicity recorded during hydraulic fracturing operations. We review the data here, and use it to understand the geological processes by which fault reactivation occurs during and after the hydraulic fracturing operations.

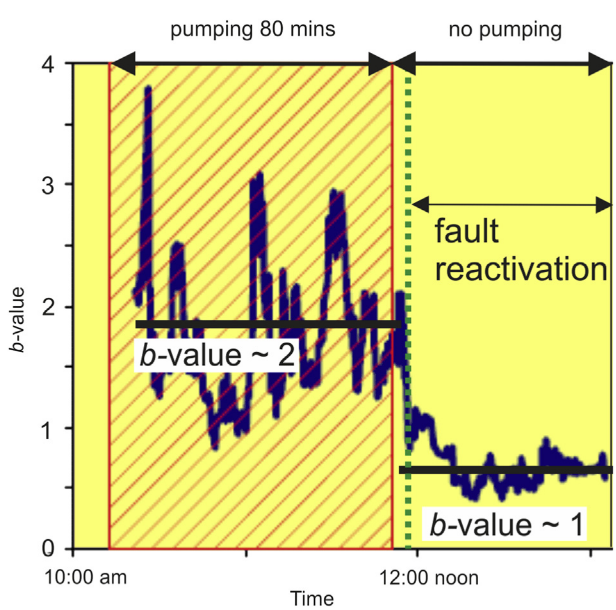

Figure 4. Detecting fault reactivation by changes in *b*-value. In this example a thrust fault was reactivated after the injection period had ended and this is marked by a change in the *b*-value from 2 to 1 (after Maxwell et al., 2009).

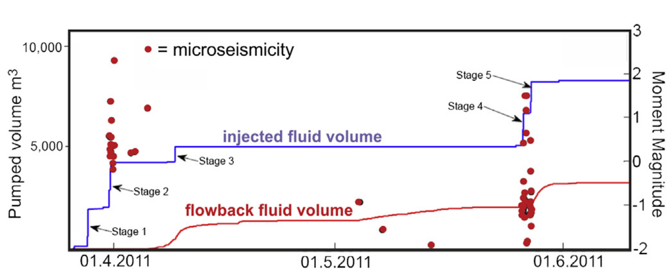

Figure 5. Pumped volume, flowback volume and moment magnitude for several microearthquakes vs. time for the Preese Hall well, drilled in 2011 in Lancashire, UK (de Pater and Baisch, 2011).

3.2. Earthquake magnitudes

Fault reactivation can cause earthquakes with magnitudes larger than expected for fracture propagation. Wolhart et al. (2005) demonstrated this in the Jonah Field in Wyoming, USA (Fig. 3). Hydraulic fracturing of the Late Cretaceous Lance Formation was carried out in a number of wells, with 9–11 hydraulic fracturing stages, using an energized borate cross-linked gel (Wolhart et al., 2005; Downie et al., 2010). The East 1 well was used for seismic measurements and the East 3 well was used for the hydraulic fracturing (Fig. 3). A graph of moment magnitude vs. distance is commonly used to identify seismicity that is anomalously large, and that clusters at specific distances from the monitoring well. Both characteristics indicate reactivation of a discrete fault (Fig. 3).

Increases in the magnitude of the microearthquakes with time following the onset of pumping are indicative of fault reactivation.

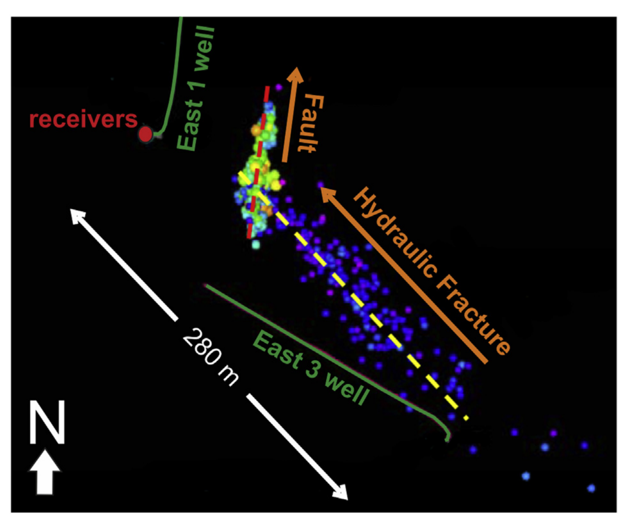

Figure 6. Microearthquakes from the Jonah Field (Wyoming, USA, location Fig. 3 inset). Blue dots: microearthquakes caused by the propagation of hydraulic fractures in East 3 well. This probably allowed fluid movement into a fault, reducing normal stress, and reactivating it (yellow and green dots). After Wolhart et al. (2005).

These have been reported to have been accompanied by a sharp reduction in *b*-value, calculated for a moving subset of events over the time that pumping took place (Maxwell et al., 2009 – Fig. 4). For example, in the case of the study of Maxwell et al. (2009), a thrust fault was penetrated by the treatment well. Sandstones offset by the fault were hydraulically fractured with a ca. 80-min-long injection. After pumping ceased, the earthquakes would be expected to reduce in size, but in this case they became larger. The *b*-value dropped from ~2 to ~1, and this was interpreted as indicating fault reactivation (Maxwell et al., 2009; Downie et al., 2010 – Fig. 4). Until recently such analyses were carried out after hydraulic fracturing was completed. However, Kratz et al. (2012) report results from the hydraulic fracturing of four horizontal wells in Montague county in Texas, in the lower Barnett shale, and propose that the *b*-values are evidence for early fault movement during and after the hydraulic fracturing.

Precursory microseismicity was not recorded in the Preese Hall well, in Lancashire, UK in 2011, where several events up to M 2.3 have been ascribed to fault reactivation (Fig. 5, Green et al., 2012). At the Preese Hall 1 well, 55 events were recorded. That the hydraulic fracturing caused fault reactivation was proposed on the basis of the unusually high magnitude and the close temporal coincidence with hydraulic fracturing stages (Fig. 5).

3.3. Spatial and temporal characteristics

Spatial clustering of the larger earthquakes can occur (Wolhart et al., 2005 – Fig. 3). Earthquakes induced at the Jonah Field, Wyoming, showed a spatial distribution that suggested new hydraulic fractures fed hydraulic fracturing fluid into a fault which consequently reactivated (Maxwell et al., 2008 – Fig. 6). The fault is approximately 200 m from the injection well.

Clustering can be temporal as well as spatial. Wessels et al. (2011) showed that for three hydraulic fracturing operations in a 24 h period there were significant increases in the normalised seismic energy emitted, and this was interpreted as discrete episodes of fault movement. Hulsey et al. (2010) describe induced strike-slip and reverse faulting in the Marcellus shale, USA, resulting from hydraulic fracturing, and characterized by short bursts of earthquakes.

Mapping hydraulic fractures in the Montney Formation, Canada, using seismicity, shows that hydraulic fractures can terminate at faults which have been mapped using 3D seismic reflection data (Maxwell et al., 2011) (Fig. 7). The edge detection map (often used

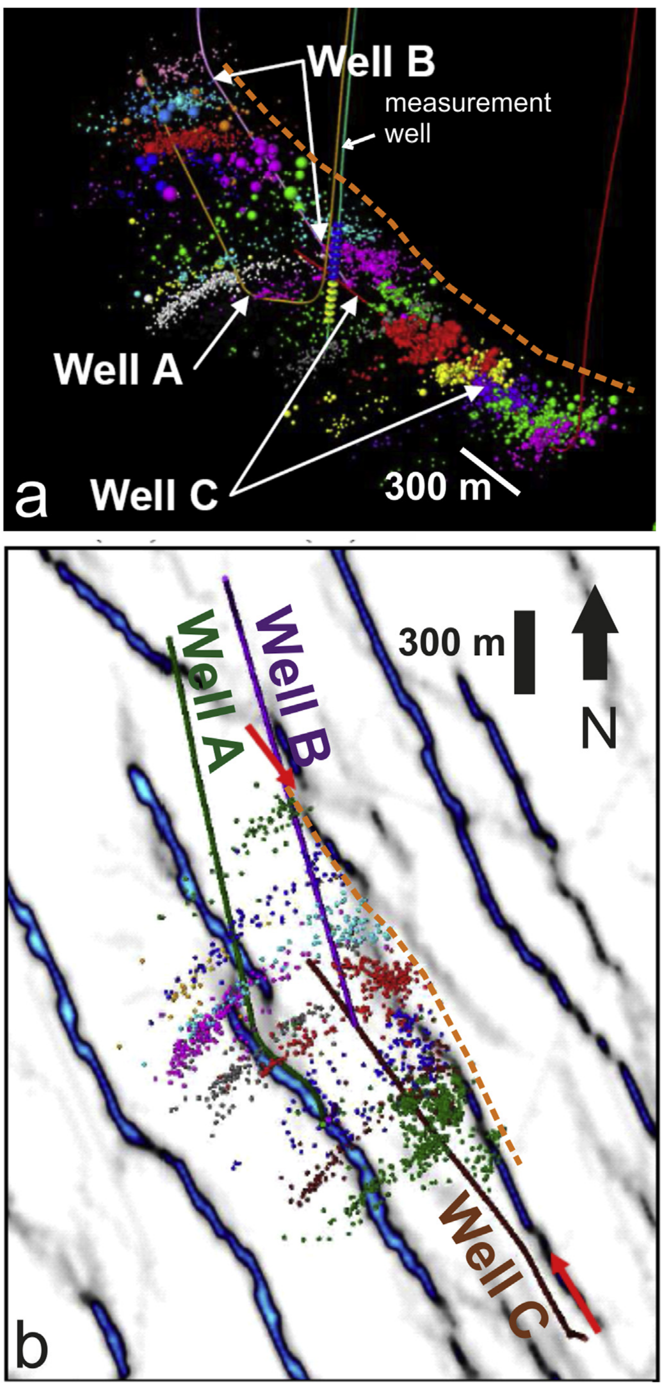

Figure 7. (a) Three wells, A, B, and C, drilled into the early Triassic upper Montney Formation in northeast British Columbia. The orange dashed line bounds the microseismicity in the northeast. (b) Edge attribute (see Brown, 2010) for a reflection in a 3D dataset over the upper Montney Formation showing NW–SE orientated faults. After Maxwell et al. (2011).

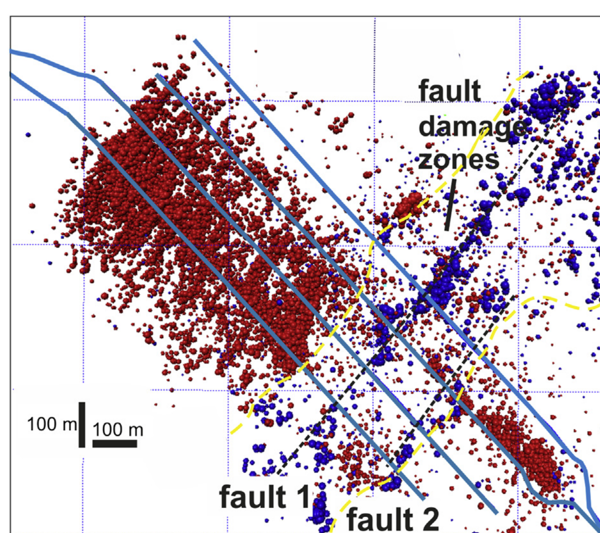

Figure 8. Map of microearthquakes induced by multiple stages of hydraulic fracturing in the Barnett shale (after Kratz et al., 2012). Blue lines – boreholes, blue dots – earthquakes with strike-slip motion, red dots – earthquakes with dip slip motion. Changes in the sense of shear on failure planes are thought to indicate a change from the stimulation of new hydraulic fractures (red dots) to fault reactivation (blue dots). Yellow-dashed lines mark interpreted extents of damage zones. This case study probably represents an example of the direct injection of fracturing fluid into a fault zone.

to identify faults in 3D seismic datasets) reveals a number of faults that trend NW–SE. The largest earthquakes located are close to a NW–SE trending fault, consistent with the interpretation that it was reactivated.

As well as injection into faults via new fractures, injection directly into faults has been recorded in the Barnett Shale (USA) (Kratz et al. (2012) (Fig. 8). The faults are strike-slip, whereas the fractures are normal. Thus, the changes in the sense of shear as well as the spatial clustering are diagnostic of fault reactivation rather than the stimulation of new fractures.

There is a growing body of research that models the process of fluid-injection-induced seismicity (e.g., Shapiro and Dinske, 2009). For example Rozhko (2010) focus on the spatial and temporal development of the microseismicity that occurs due to hydraulic fracturing and proposes that it can modelled on the basis of linear pressure diffusion in the fluid, coupled to deformation of a linear poroelastic medium. The microseismicity is considered to be caused by changes in the Coulomb yielding stress along a pressure diffusion front, caused by seepage forces (Rozhko, 2010). Geiser et al. (2012) propose that they can image extensive pre-existing fractures stimulated by these processes using a passive seismic method coined 'tomographic fracture imaging' caused by transmission of a fluid pressure pulse. The following year Lacazette and Geiser (2013) clarified that, it's not only a fluid pressure pulse but also poroelastic coupling of the stress in the rock to pore and fracture fluids could cause the stress changes without any fluid flow that stimulates fractures 100s of metres from the place where hydraulic fractures were initiated.

3.4. Long-period and long-duration events

Because of the high pressure of the hydraulic fracturing fluid, faults poorly orientated relative to the stress field may slip, but the slip may be slow and not generate conventional high-frequency microearthquakes (Das and Zoback, 2011). Das and Zoback (2011) studied 10–80 Hz, long-period, long-duration (LPLD) events

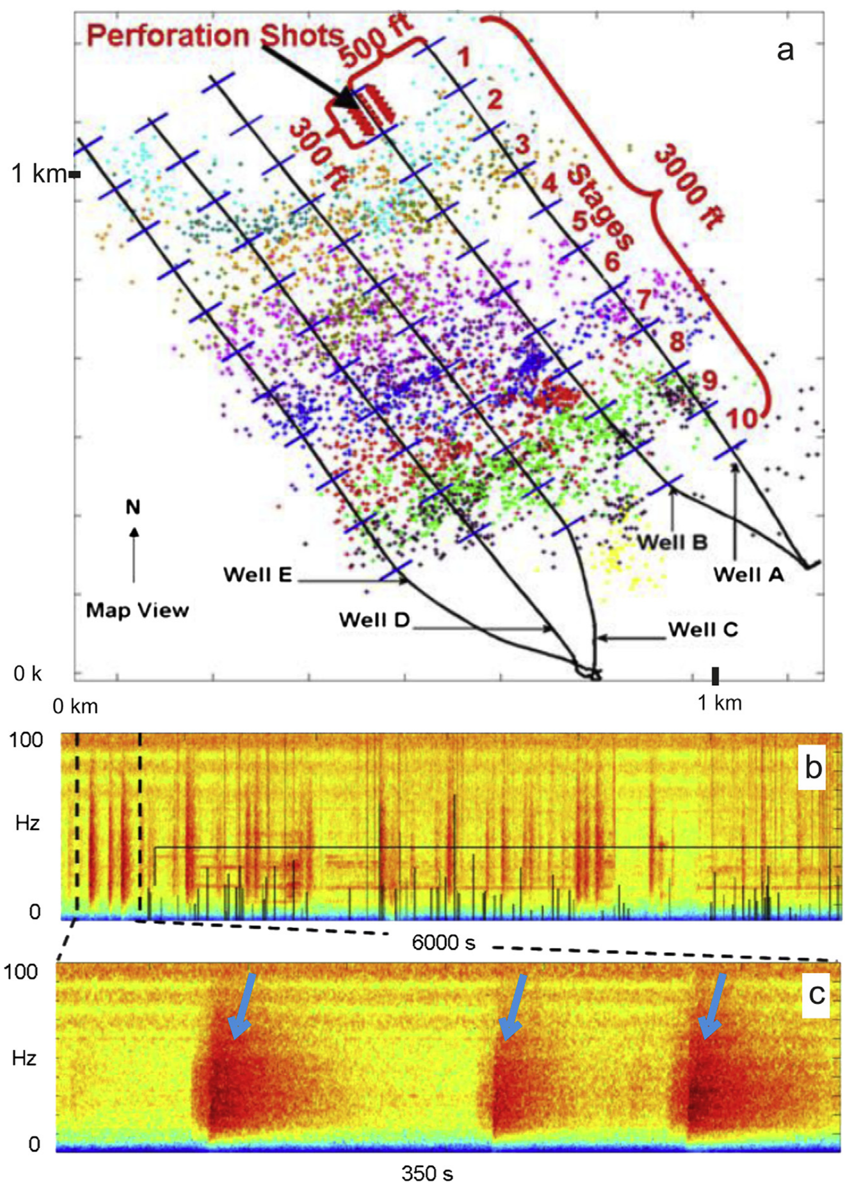

Figure 9. Long-period, long-duration (LPLD) seismicity recorded during a multi-well, multi-stage hydraulic fracturing operation in the Barnett Shale in Texas (after Das and Zoback, 2011). (a) Geometry and arrangement of wells A–E with reported seismicity. (b) Axial spectrogram of stage 7 of wells A and B revealing numerous LPLD events. (c) Examples of LPLD events observed at frequencies below 100 Hz taken from (b). Blue arrows point to the LPLD seismic events.

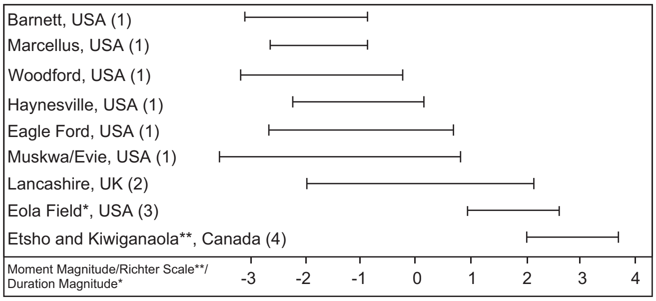

Figure 10. Comparison of reported earthquake moment magnitudes recorded in the USA, Canada and UK. (1) from Warpinski et al. (2012); (2) from de Pater and Baisch (2011); (3) from Holland (2011); (4) from the BC Oil and Gas Commission (2012).

which have similar characteristics to tectonic tremors observed in subduction zones and strike-slip plate boundaries. The maximum number of LPLD events were detected in the hydraulic fracturing stages with the highest pumping pressure and the highest natural fracture density (Fig. 9). The events were interpreted as slow shear slip on pre-existing natural fractures as a result of the high fluid pressure. The faults that moved were poorly orientated relative to the stress field.

3.5. *Nuisance seismicity*

The majority of data from the USA show that when fault reactivation occurs the earthquake magnitudes tend to be very low, and do not exceed ∼ M 1 (Fig. 10). There are three known exceptions to this, Etsho and Kiwigana, Canada in 2009, 2010 and 2011 (BC Oil and Gas Commission, 2012), the Eola Field, Oklahoma, USA in 2011 (Holland, 2011) and Lancashire, UK in 2011 (de Pater and Baisch, 2011). In 2011 a felt earthquake of magnitude M 2.3 occurred in Lancashire, UK, as a result of hydraulic fracturing of the Preese Hall well (Fig. 5). The seismicity at the Eola Field, southern Garvin County, Oklahoma, has been tentatively attributed to hydraulic fracturing. The field is characterised by a series of WNW–ESE striking faults. 43 earthquakes were located there in 2011 with magnitudes up to 2.8. Hydraulic fracturing was carried out in a number of stages and earthquakes onset 13 h after operations began (Holland, 2011).

A total of 216 earthquakes occurred 2009–2011 at the Etsho and Kiwigana fields in Horn River, Canada and 19 were between M_L 2 and 3 (Fig. 11). The largest event had a magnitude of M_L 3.8, it occurred in May 2011, and it was felt. There was a clear temporal relationship between pumping and the seismicity, with earthquakes starting several hours after the beginning of pumping (BC Oil and Gas Commission, 2012).

4. Process model

A number of conclusions can be drawn from these examples. Firstly there is evidence that faults can be connected to the injection well via hydraulic fractures (Fig. 6) as well as direct injection into faults intersecting the treatment wells (Fig. 8). Even where faults are intersected by the treatment wells, there is often a time lag of several hours between the start of pumping and fault reactivation. At the Preese Hall 1 well (Lancashire, UK), there was a delay of 10 h between cessation of pumping and the M 2.3 earthquake (de Pater and Baisch, 2011). The same observation was made by Maxwell et al. (2009) who observed a delay of approximately 80 min from the onset of pumping and evidence for fault reactivation in gas wells in Western Canada. Examples of felt seismicity documented in the Horn River, Canada occurred several hours after the start of pumping (BC Oil and Gas Commission, 2012). The delay between pumping and the reactivation of some faults (e.g., Maxwell et al., 2009) may in part be because the fault into which fluid is injected has inherent storage and transmissibility characteristics, or due to the time required for the transmission of fluid pressure by pressure diffusion and due to poroelasticity (Lacazette and Geiser, 2013).

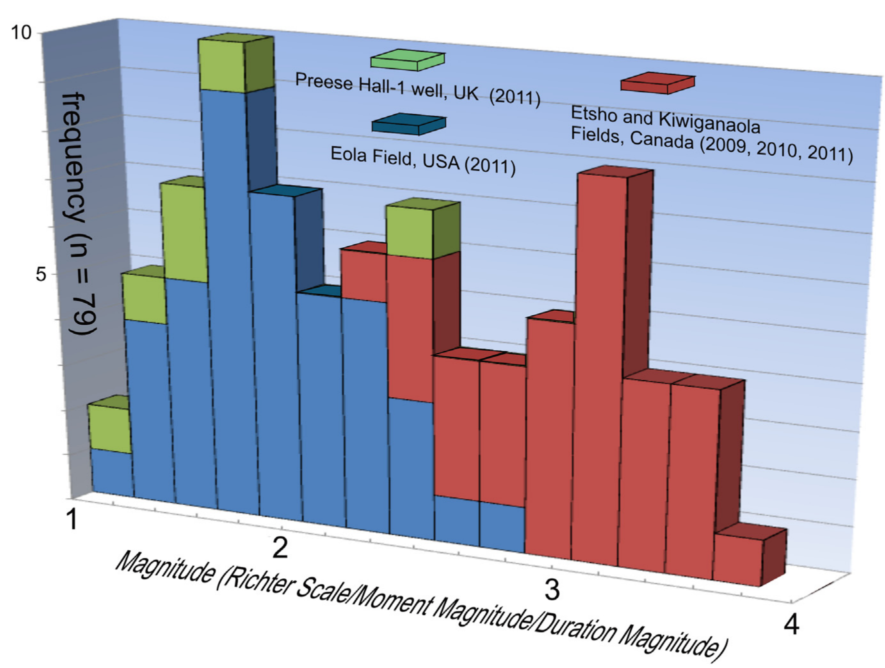

Figure 11. Range of magnitudes for the cases of felt seismicity including only magnitudes > M 1. Etsho and Kiwiganaola were reported on the M_L scale (magnitudes from Fig. 9 of BC Oil and Gas Commission, 2012), Preese Hall-1 events were recorded as moment magnitudes (de Pater and Baisch, 2011) and Eola Field, Oklahoma, USA events as duration magnitude.

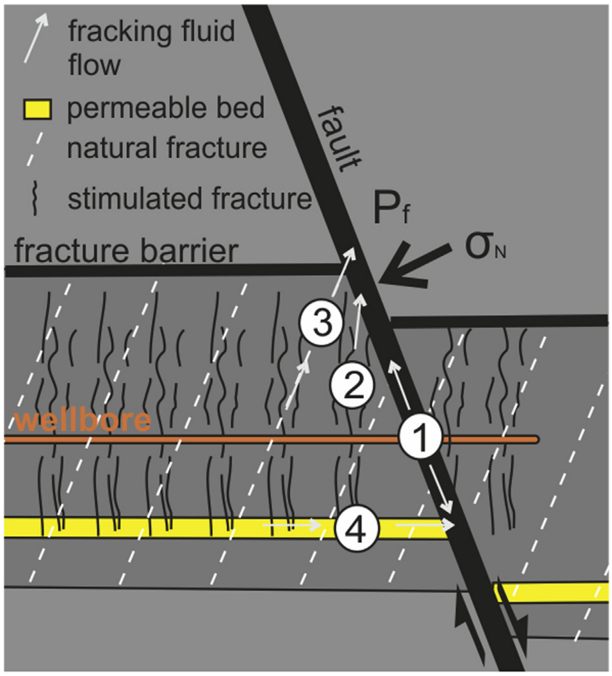

Figure 12. Cartoon of low-permeability reservoir with an intersecting fault and potential mechanisms for the transmission of a pore fluid pressure pulse or fluid into a fault to cause reactivation. 1 – Direct connection and injection into the fault (e.g., Hulsey et al., 2010); 2 – fluid flow through the stimulated hydraulic fractures into the fault (e.g., Wolhart et al., 2005); 3 – fluid flow through the existing fractures; 4 – fluid flow through permeable strata and along bedding planes.

In summary there are several mechanisms by which faults are reactivated due to hydraulic fracturing to cause felt seismicity. Fracturing fluid or displaced pore fluid could enter the fault, a fluid pressure pulse could be transmitted to the fault and due to poroelasticity, deformation or 'inflation' of the rock due to injection could increase fluid pressure in the fault or in the fractures connected to the fault (e.g. Lacazette and Geiser, 2013). The following pathways for fluid or a fluid pressure pulse are proposed: (a) directly from the wellbore; (b) through new, stimulated hydraulic fractures; (c) through pre-existing fractures and minor faults; or (d) through the pore network of permeable beds or along bedding planes (Fig. 12). The reactivated fault could be intersected by the wellbore or it could be 10s to 100s of metres from it.

5. Conclusions

Of the 198 possible examples of induced seismicity reported in the literature, magnitudes range up to M 7.9. Hydraulic fracturing of sedimentary rocks, for recovery of gas from shale, usually generates very small magnitude earthquakes only, compared to processes such as reservoir impoundment, conventional oil and gas field depletion, water injection for geothermal energy recovery, and waste water injections. We have proposed four primary mechanisms for fault reactivation by hydraulic fracturing. Although there are approaches for mitigating the risks (e.g., Brodylo et al., 2011; Green et al., 2012) and faults can often be imaged by seismic reflection data, and avoided, it cannot be ruled out that reactivation of pre-existing faults could induce felt seismicity. It should be noted, however, that after hundreds of thousands of fracturing operations, only three examples of felt seismicity have been documented. The likelihood of inducing felt seismicity by hydraulic fracturing is thus extremely small but cannot be ruled out.

Acknowledgements

We thank Durham and Keele Universities for giving the authors time to carry out this research. We thank Peter Geiser for reviewing the paper.

References

Ake, J., Mahrer, K., O'Connell, D., Block, L., 2005. Deep-injection and closely induced seismicity at Paradox Valley, Colorado. Bulletin of the Seismological Society of America 95, 664–683.

Amidzic, D., Murphy, S.K., Van Aswegen, G., 1999. Case Study of a Large Seismic Event at a South African Gold Mine, pp. 1033–1038.

Arabasz, W.J., Nava, S.J., McCarter, M.K., Pankow, K.L., Pechmann, J.C., Ake, J., McGarr, A.M., 2005. Coal-mining seismicity and ground-shaking hazard: a case study in the Trail Mountain Area, Emery County, Utah. Bulletin of the Seismological Society of America 95, 18–30.

Baisch, S., Weidler, R., Voros, R., Wyborn, D., de Graaf, L., 2006. Induced seismicity during the stimulation of a geothermal HFR reservoir in the Cooper Basin, Australia. Bulletin of the Seismological Society of America 96, 2242–2256.

Bardainne, T., Dubos-Sallée, N., Sénéchal, G., Gaillot, P., Perroud, H., 2008. Analysis of the induced seismicity of the Lacq gas field (Southwestern France) and model of deformation. Geophysical Journal International 172, 1151–1162.

Batini, F., Console, R., Luongo, G., 1985. Seismological study of Larderello — Travale geothermal area. Geothermics 14, 255–272.

BC Oil and Gas Commission, 2012. Investigation of Observed Seismicity in the Horn River Basin. <http://www.bcogc.ca/publications/reports.aspx>.

Bell, C.E., Brannon, H.D., 2011. Redesigning Fracturing Fluids for Improving Reliability and Well Performance in Horizontal Tight Shale Applications. SPE 140107.

Bennett, T.J., Marshall, M.E., Mclaughlin, K.L., Barker, B.W., Murphy, J.R., 1996. Seismic characteristics and mechanisms of rockbursts. In: Proceedings of the 18th Annual Seismic Research Symposium on Monitoring a Comprehensive Test Ban Treaty Phillips Laboratory, 153, pp. 901–907.

Bischoff, M., Cete, A., Fritschen, R., Meier, T., 2009. Coal mining induced seismicity in the Ruhr Area, Germany. Pure and Applied Geophysics 167, 63–75.

Bourouis, S., Pascal, B., 2007. Evidence for coupled seismic and aseismic fault slip during water injection in the geothermal site of Soultz (France), and implications for seismogenic transients. Geophysical Journal International 169, 723–732.

Brodylo, J., Chatellier, J.-Y., Matton, G., Rheault, M., 2011. The Stability of Fault Systems in the South Shore of St Lawrence Lowlands of Québec – Implications for Shale Gas Development. SPE 149307.

Brown, A., 2010. Interpretation of Three-dimensional Seismic Data. Tulsa, seventh ed., p. 560

Carder, D.S., 1945. Seismic investigations in the Boulder Dam area, 1940–1944, and the influence of reservoir loading on local earthquake activity. Bulletin of the Seismological Society of America 35 (4), 175–192.

Cesca, S., Dahm, T., Juretzek, C., Kühn, D., 2011. Rupture process of the 2001 May 7 Mw 4.3 Ekofisk induced earthquake. Geophysical Journal International 187, 407–413.

Chung, W.Y., Liu, C., 1992. The Reservoir-associated Earthquakes of April 1983 in Western Thailand: source modeling and implications for induced seismicity. Pure and Applied Geophysics 138, 17–41.

Cipolla, C., Maxwell, S., Mack, M., 2012. Engineering Guide to the Application of Microseismic Interpretations. SPE 152165.

Curtis, J.B., 2002. Fractured shale-gas systems. American Association of Petroleum Geologists Bulletin 86, 1921–1938.

Das, I., Zoback, M.D., 2011. Long Period, Long Duration Seismic Events During Hydraulic Fracture Stimulation of a Shale Gas Reservoir. SEG, San Antonio.

Davis, S.D., Frohlich, C., 1993. Did (or will) fluid injection cause earthquakes?: criteria for a rational assessment. Seismological Research Letters 64, 207–224.

Davis, S.D., Pennington, W.D., 1989. Induced seismic deformation in the Cogdell oil field of West Texas. Bulletin of the Seismological Society of America 79, 1477–1495.

Davis, S.D., Nyffenegger, P.A., Frohlich, C., 1995. The 9 April 1993 earthquake in south-central Texas: was it induced by fluid withdrawal? Bulletin of the Seismological Society of America 85, 1888–1895.

de Pater, C.J., Baisch, S., 2011. Geomechanical Study of Bowland Shale Seismicity. www.cuadrilla.com.

Deng, K., Zhou, S., Wang, R., Robinson, R., Zhao, C., Cheng, W., 2010. Evidence that the 2008 Mw 7.9 Wenchuan earthquake could not have been induced by the Zipingpu reservoir. Bulletin of the Seismological Society of America 100 (5B), 2805–2814.

Doser, D.I., Baker, M.R., Luo, M., Marroquin, P., Ballesteros, L., Kingwell, J., Diaz, H.L., Kaip, G., 1992. The not so simple relationship between seismicity and oil production in the Permian Basin, West Texas. Pure and Applied Geophysics 139, 481–506.

Downie, R.C., Kronenberger, E., Maxwell, S.C., 2010. Using Microseismic Source Parameters to Evaluate the Influence of Faults on Fracture Treatments – a Geophysical Approach to Interpretation. SPE 134772.

Evans, K.F., Zappone, A., Kraft, T., Deichmann, N., Moia, F., 2012. A survey of the induced seismic responses to fluid injection in geothermal and CO_2 reservoirs in Europe. Geothermics 41, 30–54.

Fritschen, R., 2009. Mining-induced seismicity in the Saarland, Germany. Pure and Applied Geophysics 167, 77–89.

Frohlich, C., Hayward, C., Stump, B., Potter, E., 2011. The Dallas-Fort Worth earthquake sequence: october 2008 through may 2009. Bulletin of the Seismological Society of America 101, 327–340.

Gahalaut, K., Gahalaut, V.K., 2010. Effect of the Zipingpu reservoir impoundment on the occurrence of the 2008 Wenchuan earthquake and local seismicity. Geophysical Journal International 183, 277–285.

Galybin, A.N., Grigovan, S.S., Mukhamediev, Sh.A., 1998. Model of Induced Seismicity Caused by Water Injection. SPE 47253, pp. 265–272.

Ge, S., Liu, M., Lu, N., Godt, J.W., Luo, G., 2009. Did the Zipingpu Reservoir trigger the 2008 Wenchuan earthquake? Geophysical Research Letters 36, L20315.

Gei, D., Eisner, L., Suhadolc, P., 2011. Feasibility of estimating vertical transverse isotropy from microseismic data recorded by surface monitoring arrays. Geophysics 76, WC117–WC126.

Geiser, P., Lacazette, A., Vermilye, J., 2012. Beyond "dots in a box": an empirical view of reservoir permeability with tomographic fracture imaging. First Break, 63–69.

Genmo, Z., Huaran, C., Shuqin, M., Deyuan, Z., 1995. Research on earthquakes induced by water injection in China. Pure and Applied Geophysics 145, 59–68.

Giardini, D., 2011. Induced Seismicity in Deep Heat Mining: Lessons from Switzerland and Europe. Presentation to National Research Council Committee on Induced Seismicity Potential in Energy Production Technologies. April 26, Washington DC.

Gibbs, J.F., Healy, J.H., Raleigh, C.B., Coakley, J., 1973. Seismicity in the Rangely, Colorado, area: 1962-1970. Bulletin of the Seismological Society of America 63, 1557–1570.

González, P.J., Tiampo, K.F., Palano, M., Cannavo, F., Fernández, J., 2012. The 2011 Lorca earthquake slip distribution controlled by groundwater crustal unloading. Nature Geoscience 5, 821–825.

Gough, D.I., Gough, W.I., 1970. Load-induced earthquakes at Lake Kariba-II. Geophysical Journal International 21, 79–101.

Grechka, V., 2010. Data-acquisition design for microseismic monitoring. The Leading Edge, 278–282.

Green, C.A., Styles, P., Baptie, B.J., 2012. Preese Hall Shale Gas Fracturing Review and Recommendations for Induced Seismic Mitigation. <http://www.decc.gov.uk/assets/decc/11/meeting-energy-demand/oil-gas/5055-preese-hall-shale-gas-fracturing-review-and-recomm.pdf>.

Gupta, H.K., 1985. The present status of reservoir induced seismicity investigations with special emphasis on Koyna earthquakes. Tectonophysics 118, 257–279.

Gupta, H.K., 2002. A review of recent studies of triggered earthquakes by artificial water reservoirs with special emphasis on earthquakes in Koyna, India. Earth-Science Reviews 58, 279–310.

Gutenberg, R., Richter, C.F., 1944. Frequency of earthquakes in California. Bulletin of the Seismological Society of America 34, 185–188.

Hamilton, J.M., Mailer, A.V., Prins, M.D., 1992. Subsidence-induced shear failures above oil and gas reservoirs. In: Tillerson, Wawersik (Eds.), Rock Mechanics. Balkema, Rotterdam.

Hanks, T., Kanamori, H., 1979. A moment magnitude scale. Journal of Geophysical Research 84, 2348–2350.

Häring, M.O., Schanz, U., Ladner, F., Dyer, B.C., 2008. Characterisation of the Basel 1 enhanced geothermal system. Geothermics 37, 469–495.

Holland, A., 2011. Examination of Possibly Induced Seismicity from Hydraulic Fracturing in the Eola Field, Garvin County, Oklahoma. Oklahoma Geological Survey Open-File Report OF1-2011.

Howe, A.M., Hayward, C.T., Stump, B.W., Frohlich, C., 2010. Analysis of recent earthquakes in Cleburne, Texas (Abstract). Seismological Research Letters 81, 379.

Hsieh, P.A., Bredehoeft, J.D., 1981. A reservoir analysis of the Denver earthquakes: a case of induced seismicity. Journal of Geophysical Research 86, 903–920.

Hubert, G., Kijko, A., Mcgarr, A., Ortlepp, W.D., 2006. Investigation into the Risks to Miners, Mines, and the Public Associated with Large Seismic Events in Gold Mining Districts.

Hulsey, B.J., Cornette, B., Pratt, D., 2010. Surface Microseismic Mapping Reveals Details of the Marcellus Shale. SPE 138806.

Jalali, M., Memarian, H., Zare, M., Dusseault, M.B., 2008. Induced Seismicity Risk in Irani Oil and Gas Fields. American Rock Mechanics Association.

Julian, B.R., Ross, A., Foulger, G.R., Evans, J.R., 1996. Three-dimensional seismic image of a geothermal reservoir: The Geysers, California. Geophysical Research Letters 23, 685–688.

Kaieda, H., Sasaki, S., Wyborn, D., 2010. Comparison of characteristics of micro-earthquakes observed during hydraulic stimulation operations in Ogachi, Hijiori and Cooper Basin HDR projects. In: Proceedings World Geothermal Congress. Bali, Indonesia, pp. 25–29.

Kanamori, H., 1977. The energy release in great earthquakes. Journal of Geophysical Research 82, 2981–2987.

Keiding, M., Árnadóttir, T., Jónsson, S., Decriem, J., Hooper, A., 2010. Plate boundary deformation and man-made subsidence around geothermal fields on the Reykjanes Peninsula, Iceland. Journal of Volcanology and Geothermal Research 194, 139–149.

Keith, C.M., Simpson, D.W., Soboleva, O.V., 1982. Induced seismicity and style of deformation at Nurek Reservoir, Tadjik SSR. Journal of Geophysical Research 87, 4609–4624.

Keranen, K.M., Savage, H.M., Abers, G.A., Cochran, E.S., in press. Potentially induced earthquakes in Oklahoma, USA: links between wastewater injection and the 2011 M w 5.7 earthquake sequence. Geology.

King, G.E., 2010. Thirty Years of Shale Gas Fracturing: What Have We Learned?. SPE 119896.

Klose, C.D., 2007. Geomechanical modeling of the nucleation process of Australia's 1989 M5.6 Newcastle earthquake. Earth and Planetary Science Letters 256, 547–553.

Kouznetsov, O., Sidorov, V., Katz, S., Chilingarian, G., 1994. Interrelationships among seismic and short-term tectonic activity, oil and gas production, and gas migration to the surface. Journal of Petroleum Science and Engineering 13, 57–63.

Kratz, M., Hill, A., Wessels, S., 2012. Identifying Fault Activation in Unconventional Reservoirs in Real Time Using Microseismic Monitoring. SPE 153042.

Kugaenko, Y., Saltykov, V., Chebrov, V., 2005. Seismic situation and necessity of local seismic monitoring in exploited Mutnovsky steam-hydrothermal field (Southern Kamchatka, Russia). In: Proceedings, World Geothermal Congress, Anatalya, Turkey, April 24–29.

Lacazette, A., Geiser, P., 2013. Comment on Davies et al 2012-hydraulic fractures: how far can they go? Marine and Petroleum Geology 43, 516–518.

Lachenbruch, A.H., Sass, J.H., 1980. Heat flow and energetics of the San Andreas fault zone. Journal of Geophysical Research 85, 6185–6222.

Lahaie, F., Boyer, E., Grasso, J.R., Fourmaintraux, D., 1998. SPHSRM Production Study as a Tool to Control the Efficiency of Reservoir Fracturing: The Lacq Case-Study. SPE 47318.

Lei, X.-L., Yu, G., Ma, S., Wen, X., Wang, Q., 2008. Earthquakes induced by water injection at ∼3 km depth within the Rongchang gas field, Chongqing, China. Journal of Geophysical Research 113, B10310.

Li, T., Cai, M.F., Cai, M., 2007. A review of mining-induced seismicity in China. International Journal of Rock Mechanics and Mining Sciences 44, 1149–1171.

Lixin, Y., Zhao, D., Liu, C.L., 2012. Preliminary study of reservoir-induced seismicity in the three Gorges Reservoir, China. Seismological Research Letters 83 (5), 806–814.

Majer, E.L., 17 November 2011. Induced Seismicity Associated with EGS Issues, Status, Challenges, Needs. Australian Geothermal Meeting, Melbourne, Australia.

Majer, E.L., Baria, R., Stark, M., Oates, S., Bommer, J., Smith, B., Asanuma, H., 2007. Induced seismicity associated with enhanced geothermal systems. Geothermics 36 (3), 185–222.

Maxwell, S.C., Shemeta, J., Campbell, E., Quirk, D., 2008. Microseismic Deformation Rate Monitoring. SPE 116596.

Maxwell, S.C., Jones, M., Parker, R., Miong, S., Leaney, S., Dorval, D., D'Amico, D., Logel, J., Anderson, E., Hammermaster, K., 2009. Fault Activation During Hydraulic Fracturing SEG Houston 2009 International Exposition and Annual Meeting 1552–1556.

Maxwell, S.C., Cho, D., Pope, T., Jones, M., Cipolla, C., Mack, M., Henery, F., Leonard, J., 2011. Enhanced Reservoir Characterisation Using Hydraulic Fracture Microseismicity. SPE 140449.

Mirzoev, K.M., Nikolaev, A.V., Lukk, A.A., Yunga, S.L., 2009. Induced seismicity and the possibilities of controlled relaxation of tectonic stresses in the Earth's crust. Physics of the Solid Earth 45, 885–904.

National Academy of Sciences, 2012. Induced Seismicity Potential in Energy Technologies.

Nicholson, C., 1992. Earthquakes associated with deep well activities- Comments and case histories. In: Wawersik, T.A. (Ed.), Rock Mechanics. A.A. Balkema, Brookfield, Vt, pp. 1079–1086.

Nicholson, C., Wesson, R.L., 1990. Earthquake Hazard Associated with Deep Well Injection. a report to the U.S. Environmental Protection Agency.

Ohtake, M., 1974. Seismic activity induced by water injection at Matsushiro, Japan. Journal of Physics of the Earth 22, 163–176.

Ottemöller, L., 2005. The 7 May 2001 induced seismic event in the Ekofisk oil field, North Sea. Journal of Geophysical Research 110, 1–15.

Pechmann, J.C., Walter, W.R., Nava, S.J., Arabasz, W.J., 1995. The February 3, 1995 ML 5.1 seismic event in the Trona Mining District of Southwestern Wyoming. Seismological Research Letters 66, 25–33.

Phillips, W.S., Rutledge, J.T., House, L.S., Fehler, M.C., 2002. Induced microearthquake patterns in hydrocarbon and geothermal reservoirs: six case studies. Pure and Applied Geophysics 159, 345–369.

Redmayne, D.W., 1988. Mining Induced Seismicity in UK Coalfields Identified on the BGS National Seismograph Network. In: Geological Society, London, Engineering Geology Special Publications, vol. 5, pp. 405–413.

Roest, J.P.A., Kuilman, W., 1994. Geomechanical Analysis of Small Earthquakes at the Eleveld Gas Reservoir. SPE 28097.

Rothé, J.P., 1970. Seismic artificiels. Tectonophysics 9, 215–238.

Rozhko, A.Y., 2010. Role of seepage forces on seismicity triggering. Journal of Geophysical Research 115, B11314.

Scholz, C.H., 1990. The Mechanics of Earthquakes and Faulting. Cambridge Univ. Press, Cambridge, p. 439.

Shapiro, S.A., Dinske, C., 2009. Fluid-induced seismicity: pressure diffusion and hydraulic fracturing. Geophysical Prospecting 57, 301–310.

Stein, S., Wiens, D.A., Fujita, K., 1982. The 1966 Kremasta reservoir earthquake sequence. Earth and Planetary Science Letters 59, 49–60.

Suckale, J., 2009. Induced seismicity in hydrocarbon fields. Advances in Geophysics 51, 55–106. (Chapter 2).

Sykes, L.R., Sbar, M.L., 1973. Intraplate earthquakes, lithospheric stresses and the driving mechanism of plate tecotnics. Nature 245, 298–302.
Vallejos, J.A., McKinnon, S.D., 2011. Correlations between mining and seismicity for re-entry protocol development. International Journal of Rock Mechanics and Mining Sciences 48, 616–625.
Van Eck, T., Goutbeek, F., Haak, H., Dost, B., 2006. Seismic hazard due to small-magnitude shallow-source, induce earthquakes in the Netherlands. Engineering Geology 87, 105–121.
Van Poollen, H.K., Hoover, D.B., 1970. Waste disposal and earthquakes at the Rocky Mountain Arsenal, Derby, Colorado. Journal of Petroleum Technology 22, 983–993.
Vulgamore, T., Clawson, T., Pope, C., Wolhart, S., Machovoe, S., Waltman, C., 2007. Applying Hydraulic Fracture Diagnostics to Optimize Stimulations in the Woodford Shale. SPE, 110029.
Warpinski, N.R., Branagan, P.T., Peterson, R.E., Wolhart, S.L., Uhl, J.E., 1998. Mapping Hydraulic Fracture Growth and Geometry Using Microseismic Events Detected by a Wireline Retrievable Accelerometer Array. SPE 40014.
Warpinski, N.R., Du, J., Zimmer, U., 2012. Measurements of Hydraulic-fracture-induced Sesimicity in Gas Shales. SPE 151597.
Wessels, S., Kratz, M., De La Pena, A., 2011. Identifying Fault Activation During Hydraulic Stimulation in the Barnett Shale: Source Mechanisms, b Values, and Energy Release Analyses of Microseismicity. In: SEG San Antonio 2011 Annual Meeting, pp. 1643–1647.
Wolhart, S.L., Harting, T.A., Dahlem, J.E., Young, T.J., Mayerhofer, M.J., Lolon, E.P., 2005. Hydraulic Fracture Diagnostics Used to Optimize Development in the Jonah Field. SPE 102528.
Zhong, Y.Z., Gao, C.B., Bai, Y., 1997. Induced seismicity in Liaoning Province, China. Pure and Applied Geophysics 150, 461–472.
Zoback, M.D., Harjes, H.-P., 1997. Injection-induced earthquakes and crustal stress at 9 km depth. Journal of Geophysical Research 102, 18,477–18,491.
Zoback, M.D., Hickman, S., 1982. In Situ study of the physical mechanisms controlling induced seismicity. Journal of Geophysical Research 87, 6959–6974.